# Model-based investigation of elasticity and spectral exponent from atomic force microscopy and electrophysiology in normal versus Schizophrenia human cerebral organoids

Anirban Dutta, John Biber, Yongho Bae, Justyna Augustyniak, Michal Liput, Ewa Stachowiak, Michal K. Stachowiak

Abstract—The physiological origin of the aperiodic signal present in the electrophysiological recordings, called 1/f neural noise, is unknown; nevertheless, it has been associated with health and disease. The power spectrum slope,  $-\alpha$  in  $1/f^{\alpha}$ , has been postulated to be related to the dynamic balance between excitation (E) and inhibition (I). Our study found that human cerebral organoids grown from induced pluripotent stem cells (iPSCs) from Schizophrenia patients (SCZ) showed structural changes associated with altered elasticity compared to that of the normal cerebral organoids. Furthermore, mitochondrial drugs modulated the elasticity in SCZ that was found related to the changes in the spectral exponent. Therefore, we developed an electro-mechanical model that related the microtubular-actin tensegrity structure to the elasticity and the  $1/f^{\alpha}$  noise. Modelbased analysis showed that a decrease in the number and length of the constitutive elements in the tensegrity structure decreased its elasticity and made the spectral exponent more negative while thermal white noise will make  $\alpha$ =0. Based on the microtubularactin model and the cross-talk in structural (elasticity) and functional (electrophysiology) response, aberrant mitochondrial dynamics in SCZ are postulated to be related to the deficits in mitochondrial-cytoskeletal interactions for long-range transport of mitochondria to support synaptic activity for E/I balance.

Clinical Relevance—Our experimental data and modeling present a structure-function relationship between mechanical elasticity and electrophysiology of human cerebral organoids that differentiated SCZ patients from normal controls.

### I. INTRODUCTION

Brain organoids are self-assembled 3D structures in vitro that can model neurodevelopment of the human brain [1], including its structure and function in health and disease [2]. Diffusion magnetic resonance imaging of human brain has shown that the cerebral fiber pathways form a rectilinear 3D grid with the correlated adaptation of structure and function [3]. The rectilinear 3D grid can be modeled as tensegrity structures that can sense and respond [4]. These cellular tensegrity structures are composed of an interconnected network of actin microfilaments and microtubules that hold the cell surface under stress in a tensegrity model [5]. Here, it can

be postulated that the cell surface provides the spatiotemporal input (dendritic spine) and readout (synaptic bouton) that can be dynamically organized by the tensegrity structure with memristor like elements [6], which can provide computational complexity to a single neuron [7]. Then, the synaptic cargo transport along the cytoskeletal highway are dynamically arranged by the cytoskeleton activity [8] for excitatory (E) and inhibitory (I) synaptic activity [9] (and E/I balance) that is powered by mitochondrial bioenergetics [10]. Here, mitochondrial network is postulated to represent a complex, self-organized system at the edge of instability [11]. Then, adenosine triphosphate (ATP) levels determine temporal fluctuations of large intracellular particles and the mechanical work by the cytoskeleton [8] that support the synaptic activity and its reorganization by microtubules [9] nucleated from the microtubule-organizing centers - centrosome, etc. So, a cellular structure-function relationship can be postulated where the cytoskeletal structure determines cell's dynamic modulus as well as electrophysiology. Published mathematical formulation [5] have shown frequency-dependent component of the cell's dynamic modulus. The observed power-law frequency-dependence of the moduli was explained by soft glassy rheology (SGR) that can be modeled by an effective (noise) temperature and characterized by structural disorder and metastability [12]. The tensegrity model can be combined with SGR, where the prestress in the tensegrity structure reduces the effective temperature of the cytoskeleton and modulates the power-law material behavior [13]. Here, the effective noise temperature for the viscoelastic response of the network is ATP-related [14]. So, the cytoskeleton is a nonequilibrium composite material [14] with self-organized criticality and dynamic instability from microtubule growth, i.e., distribution of the nucleated site lengths obey an algebraic power-law relationship [15]. Here, site nucleated microtubules follow a distribution with frequency-dependent elastic modulus [13] that determine the stiffness matrix of the cellular tensegrity structure interfacing with the cytosol with complex interfacial properties that will require detailed computational modeling [16] for elucidation.

 $^*$  Funding for the experiments provided by NSF grants, CBET-1706050 and CBET-2039189. J. Augustyniak was funded by the National Science Center (ETIUDA 6 no. 2018/28/T/NZ3/00525).

J. Biber was with the University at Buffalo, NY 14260 USA.

Y. Bae was with the University at Buffalo, NY 14260 USA.

J. Augustyniak was with the University at Buffalo, NY 14260 USA and Department of Neurochemistry, Mossakowski Medical Research Institute, Polish Academy of Sciences, Warsaw, Poland.

M. Liput was with the University at Buffalo, NY 14260 USA.
E. Stachowiak was with the University at Buffalo, NY 14260 USA.
M. K. Stachowiak is with the University at Buffalo, NY 14260 USA.
A. Dutta was with the University at Buffalo, NY USA (corresponding author phone: (716) 645-9161; e-mail: anirband@buffalo.edu).

In this study, we investigated the power-law behavior of electrically polar intracellular materials, including microtubules [17] and organelles [18], that can be related to the quasi-periodic external electric potential both in space and time [19]. Prior work [20] showed spontaneous changes in the oscillatory behavior of patched microtubule bundles, where 39 Hz was the fundamental frequency. Then, the electric field in mitochondria with transmembrane potential of ~150mV across ~5nm membrane thickness can be 3e+7 V/m where mitochondria and microtubules form a unique cooperating electrodynamic system in the cell [21]. Considering a percolation matrix for the organized mitochondria [11] at a population level with spatial degrees of freedom, a selforganized critical (SOC) dynamics can give rise to  $1/f^{\alpha}$  decay relationship [22] with discrete, impulsive events spanning a broad range of sizes (i.e., crackling noise). This crackling noise will be reflected in the structure (vibration) and function (electrophysiology) that is likely to be independent of microscopic and macroscopic details [23]. Therefore, simple models can be used for the hyperuniversality (power-law exponents are independent of the scale [22]) that can provide systems-level insight in to health and disease. So, the current study aimed to investigate the electro-mechanical connection in human cerebral organoids from normal subjects and schizophrenia patients using electrophysiology and atomic force microscopy. In our prior work [10], we showed a relationship between the synaptic E-I ratio based on the spectral exponent ( $-\alpha$  in  $1/f^{\alpha}$ ) of local field potentials and the activity of mitochondrial Cytochrome-C Oxidase. Here, we postulate that the difference in the power spectrum slope between normal and schizophrenia organoids, shown related to bioenergetics [10], can also be related to the difference in the elastic modulus – an electro-mechanical connection.

### II. METHODS

### A. Cerebral organoids for phase zero study

Two commercial healthy (normal) control cell lines (23,476\*C: Female and 3651: Female) and the two commercial schizophrenic cell lines (1835: Female and 1792: Male) were chosen that displayed maldevelopment of the cortical structures in cerebral organoids in our prior work on schizophrenia neurodevelopment in [2, p. Neurosperes/neuroepithelium (with visible bright marginal zones) were embedded in Matrigel droplets and transferred to 6 cm plates in cerebral organoid media without vitamin A for 4 days, followed by transfer to an orbital shaker and in cerebral organoid media with vitamin A. After 10 days in the shaker (14 days after Matrigel embedding), the cerebral organoids were treated with (a) vehicle (control), (b) Idebenone (IDB), (c) Lipoic acid + Acetyl L-carnitine (LC+LA), and (d) Choline (CHO). Media was changed every 2 days, and then the cerebral organoids at various timepoints of maturity were embedded to the center of 3.5 cm plate using Matrigel, and the experimental multi-modal recordings were performed [10].

### B. 32-channel electrophysiology

The left panel of Figure 1 shows an adjustable tetrode depth array for 32-channel electrophysiology from Matrigel embedded brain organoid [10]. A 32-channel Intan RHD2132 amplifier (Intan Technologies, USA) and OpenEphys data acquisition system were used for electrophysiology. Intan RHD2132 amplifier (Intan Technologies, USA) supported

sampling 32 amplifier channels at 30 kSamples/s each and provided a fully integrated electrophysiology amplifier array with an on-chip 16-bit analog-to-digital converter (ADC). Open Ephys acquisition board read 8 Intan amplifiers, i.e., in 8 multi-well bioreactor chips, using low-voltage differential signaling connected to the computer's USB port. We used the OpenEphys GUI and the LFP viewer and Spike Detector plugins to record in the fault-tolerant OpenEphys data format in blocks of 1024 samples, each of which included a timestamp and a readily identifiable 'record marker' [10].

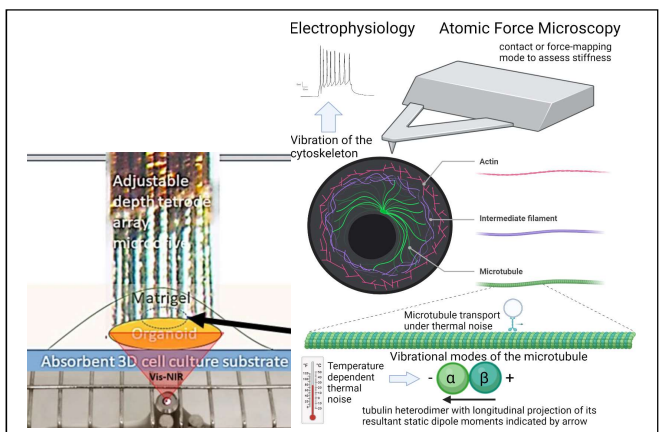


**Figure 1.** Left Panel: Electrophysiology in conjunction with Vis/NIR spectroscopy from prior work [19]. Right Panel: Cytoskeletal electro-mechanical behavior from electrophysiology and atomic force microscopy. Disruption of microtubules bearing compressive forces leads to substrate traction from tensed actin and microfilaments [8] and cross-talk, i.e., changes the electromechanical behavior. Created with BioRender.com

# C. Atomic force microscopy (AFM)

The right panel of Figure 1 shows our concept for measuring electro-mechanical responses of the cerebral organoids. The organoids were adhered to 18mm glass coverslips by dispensing single suspended organoids on a 2-5  $\mu l$  droplet of Matrigel and incubating them to dry at 37°C for 15 minutes and hydrating the adherent organoids with serum-containing growth medium. Force-Distance (F/D) curves were obtained by indenting the outer membrane of the organoids in contact mode to assess organoid elastic modulus using a Park Systems NX-12 AFM. F/D curves were analyzed using XEI software (Park Systems) to quantify the elastic modulus of the organoids. The first 400-600 nm of tip deflection were fitted with the Hertz model for a cone. Finally, these force curves were analyzed and converted to Young's moduli.

### D. Computational model

Mitochondria are the source of internal heat and biophotons, i.e., thermal noise, that can lead to fluctuations of microtubules between coherent and incoherent states [24]. Then, elasto-electrical vibrations and dynamics of microtubules can generate oscillatory electric field [25] where multi-mode vibration can also generate an electric field in the form of an electric pulse [19]. To simplify this complex nonlinear dynamical system, we specifically focused on a lumped model that can explain  $1/f^\alpha$  'noise'. Modal analysis of the cytoskeletal structure for small deformation, performed

with tapping mode AFM, can provide insights into its response spectrum. Here, the dynamic modulus,  $E_T$ , is frequency dependent [5], that can be decomposed into elastic and dissipative components,  $E_T = E_E + iE_D$  (*i* is the imagery unit). The ratio,  $\frac{E_D}{E_E}$ , depends on the rheological properties that determine relative dissipation of the energy, modeled by the quality factor, Q, of a harmonic oscillator with resonant frequency,  $\omega_0$  [19] that may capture health versus disease state, e.g., dissipation or loss of energy [8] is postulated to be low in health. Here, a combination of N 'not overdamped' oscillators in the frequency domain is given by [19],  $H_N =$  $\frac{1}{N}\sum_{k=1}^{N} \frac{i\frac{\omega}{Q_k}}{\omega_{0k} + i\frac{\omega}{Q_k} - \frac{\omega^2}{\omega_{0k}}}.$  The energy [8] due to quadratic mean thermal vibration at the n<sup>th</sup> resonant frequency is given by,  $2k_BT^*\frac{B_n}{\omega_{0n}\varrho_n}|H_N(\omega_{0n})|^2$ , where  $B_n=\frac{\omega_{0n}}{4\varrho_n}$  is the effective noise bandwidth of the n<sup>th</sup> resonance,  $k_B$  is the Boltzmann constant, and  $T^*$  is the temperature [19]. Here, axial Young modulus of the microtubule is around 0.1 kPa, temperature 300K [19]. Then, tensegrity model stiffness (stiffness= $\frac{E_a A}{c}$ ). axial Young's modulus,  $E_a$ , cross-sectional area, A ,and length, L) and local properties of the constitutive components have constant relationships [26]; captured by a unique nondimensional parameter,  $R = \frac{T^{0.5}}{N^{2.7}(L)^2}$ , to estimate the normalized elasticity modulus where T is normalized prestress, N is normalized number, and L is normalized length of the constitutive elements. This parameter, R, remains valid as the tensegrity model scales from cytoskeleton to cellextracellular matrix (ECM) structure, i.e., universality. Here, increasing the number and increasing the length of the microtubules both softens to a similar extent whereas the structure becomes stiffer when the internal tension (actin) is increased. Then, self-organized criticality (SOC) [15] can generate  $1/f^{\alpha}$  'noise' in the electrophysiology signal due to the formation of trapping sites at the nucleating microtubules [19] for the propagating electric pulses on the microtubule network. The probability of 'm' such electric pulses in time interval, 't,' can be given by  $p(m,t) = \frac{(\vartheta t)^m}{m!} e^{-\vartheta t}$  where  $\vartheta$  is the mean rate of transition from microtubule to microtubule per second. If we consider discrete states, 1 and 0, for transition and trapping of the electric pulse then the time in those states are exponentially distributed and the switching between the states is a Poisson process. Here, reduced L and N can reduce the lifetime of the trapping events [22]. Then, dissipation of the pulse energy can lead to its exponential decay [19]. So, this multi-scale directional propagation dynamics of  $\delta$ -correlated (due to dissipation) uniform random noise on dynamic tensegrity lattices with dissipative SOC gives rise to 1/f<sup>\alpha</sup> 'noise' [22]. Here, there are two components, the energy injection in order to activate all the lattice [22] whereas pulse propagation can become quickly inactive with energy (ATP)

# considered anomalous or non-ergodic diffusion process [8]. III. RESULTS

depletion, e.g. in the diseased state [27]. This can be

Figure 2A shows the elastic modulus from AFM analysis on the surface of the cerebral organoids from normal (Control) and Schizophrenia treated with mitochondrial drugs; vehicle treatment (-), Idebenone (IDB), Lipoic acid+Acetyl L-

carnitine (LC+LA), and Choline (CHO). The elastic modulus of Schizophrenia cerebral organoids is dramatically increased compared to control cerebral organoids (Fig. 2A; columns 1 and 2). The increased elastic modulus (reduced elasticity) of the schizophrenia organoids was reversed by combined mitochondrial drugs acetyl L-Carnitine plus Lipoic Acid (Fig. 2A; column 5) but not by a single treatment with Choline (Fig. 2A; column 3) or Idebenone (Fig. 2A; column 4). Figure 2B shows the mean slope of the power spectrum, also called the spectral exponent, across all tetrode channels of the electrophysiological recordings from 34 days old organoid surface of Schizophrenia patients treated with vehicle (-), IDB, LC+LA, and CHO. We observed that higher elastic modulus led to a more negative spectral exponent. Specifically, while IDB increased the elastic modulus and made the spectral exponent more negative than that with the vehicle treatment, both CHO and LC+LA decreased the elastic modulus, which corresponded with less negative spectral exponent than that with vehicle treatment. We developed a six-strut tensegrity model [13], shown in Figure 3A, with a cell-mimetic (radius 6.8 µm) mass matrix (3C) and stiffness matrix (3D) that resulted in natural frequencies (3B) in MHz. Here, for a sixstrut tensegrity cell model [13], cell elasticity,  $E \approx \frac{T_a^0 \phi_a}{3} \approx$  $\frac{T_m^0 \phi_m}{3}$ , where  $T_a^0$  and  $T_m^0$  are prestress while  $\phi_a$  and  $\phi_m$  are relative density of the actin cables and microtubule struts respectively. For  $T_a^0 = 1 \times 10^6 \ Pa$ ,  $T_m^0 = 1 \times 10^5 \ Pa$ ,  $\emptyset_a = 1 \times 10^6 \ Pa$ 0.21%,  $\phi_m = 0.19$ %, we find  $E_{max} \approx \frac{1 \times 10^6 \times 0.21}{3 \times 100} \approx 0.7 \times 10^{-10}$ 10<sup>3</sup> Pa comparable 'Control' organoid value in Figure 2A.

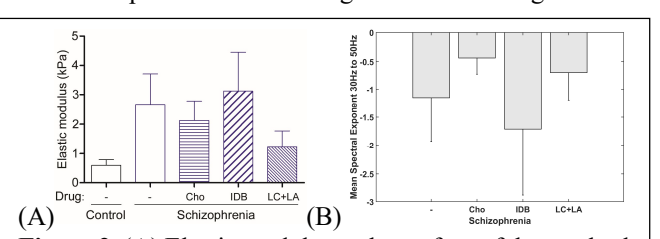


**Figure 2.** (A) Elastic modulus at the surface of the cerebral organoid. (B) Mean spectral exponent  $(-\alpha \text{ in } 1/f^{\alpha})$  across all 32 electrodes at the surface of cerebral organoid. The stiffness and mean spectral exponent of schizophrenia cerebral organoid treated with or without drugs (Choline, Cho; Idebenone, IDB; acetyl L-Carnitine+ Lipoic Acid, LC+LA) was compared to control cerebral organoid. Graphs show mean + SEM.

# IV. DISCUSSION

Cerebral organoids grown from induced pluripotent stem cells (iPSCs) from patients with Schizophrenia (SCZ) recapitulate cortical malformations [2] that were reflected in altered elastic modulus compared to that of control cerebral organoids as measured by AFM (Figure 2A). Then, drugs affected the SCZ organoid's structural (elastic modulus) and functional (spectral exponent) characteristics. Here, IDB is known for its distinct effects on the bioenergetics of cortical neurons [28] that increased elastic modulus and mean spectral exponent that underlies information processing capacity (i.e., E/I balance [10]). An increased elastic modulus can be related to a decrease in the number (N) and length (L) of the

constitutive elements of the tensegrity structure  $(R = \frac{1}{N^{2.7}(L)^2})$  [17]. Here, reduced L and N, e.g., in aberrant microtubule nucleation [29], can reduce the lifetime of the trapping events [22], thereby making the spectral exponent more negative. The proposed electrical pulse propagation analysis can also be applied to synaptic vesicle precursors where reduced L acting as roadblocks can increase the time required for transport that can be a single rate-constant model [30]. Therefore, microtubule dynamics is implicated in neuronal excitability [29], so we propose that  $1/f^{tx}$  neural noise, related to E/I balance, is determined by microtubule dynamics and cytoskeletal components that determine the elastic modulus.

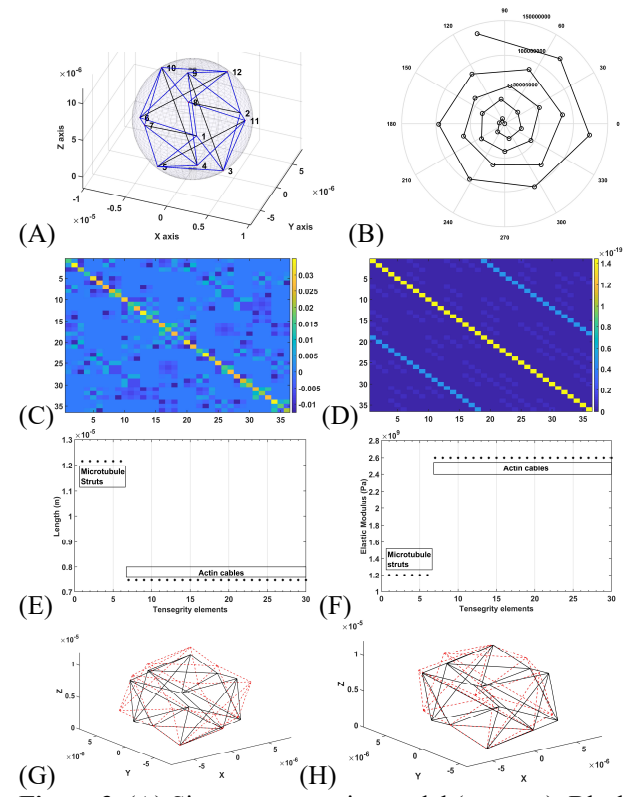


**Figure 3.** (A) Six-strut tensegrity model (axes: m). Black lines: actin tension cables. Blue compression struts: microtubules. (B) Polar plot of natural frequency response (radius: Hz). (C) Stiffness (colorbar: N/m) matrix. (D) Mass (colorbar: kg) matrix. (E) Length (in m) of the microtubule struts (x6) and actin tension cables (x24). (F) Elastic modulus (in Pa) of the microtubule struts (x6) and actin tension cables (x24). (G) First and (H) Second mode.

Furthermore, an adaptation of the microtubule dynamics and the cytoskeletal components can underlie a physical neural network [31] at a single neuron level that needs further investigation. This physical neural network extends from a single neuron to a multi-neuronal network in the brain. Here, disruption of cortical layers and connectivity of cortical neurons in SCZ [2], related to dysfunctional cell migration during neurodevelopment, can also be due to dysfunctional microtubules [32]. Since dendritic branches can be considered as a set of spatiotemporal pattern detectors [8], shaping the multi-neuronal network by cytoskeleton will be crucial during neurodevelopment for normal information processing

capacity. Electromagnetic energy injection can activate all the lattice system, where microtubular response has been shown affected also by the magnitude and polarity of the stimulus [20]. For example, spontaneous microtubule growth may be responsive to electromagnetic pumping [33] that needs investigation in 'phase zero' and in vivo neurodevelopmental studies [27]. Also, 39 Hz stimulation at the fundamental frequency of the patched microtubule bundles needs investigation vis-à-vis its role in synchronous rhythmic firing of neurons to reduce amyloid plaques [34]. Then, microtubule [29] nucleation during photobiomodulation investigation to model a decrease in the spectral exponent with an increase in mitochondrial Cytochrome-C Oxidase found in our prior work [35]. Then, interruption of microtubule polymerization by electric field 1-2 V/m in the 100-300 kHz frequency range [21], e.g., for cancer treatment, may be feasible with non-invasive deep brain stimulation [36]. Here, resonant frequencies of the subcellular tensegrity structure is postulated to be crucial, e.g., mechanical and electromagnetic oscillations responsive to microtubule nano-oscillators [21] may overlap [19]. Also, the cytoskeletal structure is likely adapted with its in vivo environment for controlled physical transformations during learning [31], e.g., postulated ultrafast physical reservoir computing [7]. Therefore, investigation of the cytoskeletal-ECM structural dynamics during information processing, and its plasticity and bioenergetics (e.g., in ATP depletion [27]) is crucial in health and disease.

### ACKNOWLEDGMENT

AD developed the concept, performed the computational modeling and the electrophysiology study. JB and YB performed and analyzed the AFM data, JA, ML developed the cerebral organoids and drug treatment under ES supervision. AD, YB, and MKS reviewed the experimental findings. The experimental data and the computational models are available at the https://www.brainrhythm.org/.

### REFERENCES

- [1] C. A. Trujillo and A. R. Muotri, "Brain organoids and the study of neurodevelopment," *Trends Mol Med*, vol. 24, no. 12, pp. 982–990, Dec. 2018, doi: 10.1016/j.molmed.2018.09.005.
- [2] E. K. Stachowiak et al., "Cerebral organoids reveal early cortical maldevelopment in schizophrenia—computational anatomy and genomics, role of FGFR1," Transl Psychiatry, vol. 7, Nov. 2017, doi: 10.1038/s41398-017-0054-x.
- [3] V. J. Wedeen *et al.*, "The Geometric Structure of the Brain Fiber Pathways," *Science*, vol. 335, no. 6076, pp. 1628–1634, Mar. 2012, doi: 10.1126/science.1215280.
- [4] D. E. Ingber, "Tensegrity: the architectural basis of cellular mechanotransduction," *Annu Rev Physiol*, vol. 59, pp. 575–599, 1997, doi: 10.1146/annurev.physiol.59.1.575.
- [5] N. Wang et al., "Mechanical behavior in living cells consistent with the tensegrity model," PNAS, vol. 98, no. 14, pp. 7765–7770, Jul. 2001, doi: 10.1073/pnas.141199598.
- [6] J. A. Tuszynski et al., "Microtubules as Sub-Cellular Memristors," Sci Rep, vol. 10, no. 1, p. 2108, Feb. 2020, doi: 10.1038/s41598-020-58820-y.
- [7] D. Beniaguev, I. Segev, and M. London, "Single cortical neurons as deep artificial neural networks," *Neuron*, vol. 109, no. 17, pp. 2727-2739.e3, Sep. 2021, doi: 10.1016/j.neuron.2021.07.002.

- [8] I. Wohl and E. Sherman, "Spectral Analysis of ATP-Dependent Mechanical Vibrations in T Cells," Frontiers in Cell and Developmental Biology, vol. 9, 2021, Accessed: Jan. 14, 2022. [Online]. Available: https://www.frontiersin.org/article/10.3389/fcell.2021.59065
- [9] J. Parato and F. Bartolini, "The microtubule cytoskeleton at the synapse," *Neurosci Lett*, vol. 753, p. 135850, May 2021, doi: 10.1016/j.neulet.2021.135850.
- [10] A. Dutta et al., "A proof of concept 'phase zero' study of neurodevelopment using brain organoid models with Vis/near-infrared spectroscopy and electrophysiology," Scientific Reports, vol. 10, no. 1, Art. no. 1, Dec. 2020, doi: 10.1038/s41598-020-77929-8.
- [11] M. A. Aon, S. Cortassa, and B. O'Rourke, "Percolation and criticality in a mitochondrial network," *Proc Natl Acad Sci U S A*, vol. 101, no. 13, pp. 4447–4452, Mar. 2004, doi: 10.1073/pnas.0307156101.
- [12] K. K. Mandadapu, S. Govindjee, and M. R. K. Mofrad, "On the cytoskeleton and soft glassy rheology," *Journal of Biomechanics*, vol. 41, no. 7, pp. 1467–1478, Jan. 2008, doi: 10.1016/j.jbiomech.2008.02.014.
- [13] D. E. Ingber, N. Wang, and D. Stamenović, "Tensegrity, cellular biophysics, and the mechanics of living systems," *Rep Prog Phys*, vol. 77, no. 4, p. 046603, Apr. 2014, doi: 10.1088/0034-4885/77/4/046603.
- [14] D. Mizuno, C. Tardin, C. F. Schmidt, and F. C. MacKintosh, "Nonequilibrium Mechanics of Active Cytoskeletal Networks," *Science*, Jan. 2007, doi: 10.1126/science.1134404.
- [15] P. Babinec and M. Babincová, "Self-organized criticality and dynamic instability of microtubule growth," Z Naturforsch C J Biosci, vol. 50, no. 9–10, pp. 739–740, Oct. 1995, doi: 10.1515/znc-1995-9-1024.
- [16] S. A. Fiorenza, D. G. Steckhahn, and M. D. Betterton, "Modeling spatiotemporally varying protein-protein interactions in CyLaKS, the Cytoskeleton Lattice-based Kinetic Simulator," *Eur Phys J E Soft Matter*, vol. 44, no. 8, p. 105, Aug. 2021, doi: 10.1140/epje/s10189-021-00097-8.
- [17] A. Mershin, A. A. Kolomenski, H. A. Schuessler, and D. V. Nanopoulos, "Tubulin dipole moment, dielectric constant and quantum behavior: computer simulations, experimental results and suggestions," *Biosystems*, vol. 77, no. 1–3, pp. 73–85, Nov. 2004, doi: 10.1016/j.biosystems.2004.04.003.
- [18] A. Saminathan et al., "A DNA-based voltmeter for organelles," Nat. Nanotechnol., vol. 16, no. 1, Art. no. 1, Jan. 2021, doi: 10.1038/s41565-020-00784-1.
- [19] D. Havelka, M. Cifra, and O. Kučera, "Multi-mode electro-mechanical vibrations of a microtubule: In silico demonstration of electric pulse moving along a microtubule," *Appl. Phys. Lett.*, vol. 104, no. 24, p. 243702, Jun. 2014, doi: 10.1063/1.4884118.
- [20] M. del R. Cantero, C. Villa Etchegoyen, P. L. Perez, N. Scarinci, and H. F. Cantiello, "Bundles of Brain Microtubules Generate Electrical Oscillations," *Sci Rep*, vol. 8, no. 1, p. 11899, Aug. 2018, doi: 10.1038/s41598-018-30453-2.
- [21] J. Pokorný, "Physical aspects of biological activity and cancer," AIP Advances, vol. 2, no. 1, p. 011207, Mar. 2012, doi: 10.1063/1.3699057.
- [22] P. De Los Rios and Y.-C. Zhang, "Universal \$1/mathit{f}\$ Noise from Dissipative Self-Organized Criticality Models," *Phys. Rev. Lett.*, vol. 82, no. 3, pp. 472–475, Jan. 1999, doi: 10.1103/PhysRevLett.82.472.

- [23] J. P. Sethna, K. A. Dahmen, and C. R. Myers, "Crackling noise," *Nature*, vol. 410, no. 6825, Art. no. 6825, Mar. 2001, doi: 10.1038/35065675.
- [24] M. Rahnama, J. A. Tuszynski, I. Bókkon, M. Cifra, P. Sardar, and V. Salari, "Emission of mitochondrial biophotons and their effect on electrical activity of membrane via microtubules," *J Integr Neurosci*, vol. 10, no. 1, pp. 65–88, Mar. 2011, doi: 10.1142/S0219635211002622.
- [25] M. Cifra, J. Pokorný, D. Havelka, and O. Kučera, "Electric field generated by axial longitudinal vibration modes of microtubule," *Biosystems*, vol. 100, no. 2, pp. 122–131, May 2010, doi: 10.1016/j.biosystems.2010.02.007.
- [26] S. Wendling, P. Cañadas, and P. Chabrand, "Toward a Generalised Tensegrity Model Describing the Mechanical Behaviour of the Cytoskeleton Structure," *Computer Methods in Biomechanics and Biomedical Engineering*, vol. 6, no. 1, pp. 45–52, Feb. 2003, doi: 10.1080/1025584021000059413.
- [27] S. S. Karanth, R. Mujumdar, J. P. Sahoo, A. Das, M. K. Stachowiak, and A. Dutta, "Human Brain Organoid Platform for Neuroengineering Optical Theranostics in Neonatal Sepsis," in *Converging Clinical and Engineering Research on Neurorehabilitation IV*, Cham, 2022, pp. 753–757. doi: 10.1007/978-3-030-70316-5 120.
- [28] S. M. Jaber, S. X. Ge, J. L. Milstein, J. W. VanRyzin, J. Waddell, and B. M. Polster, "Idebenone Has Distinct Effects on Mitochondrial Respiration in Cortical Astrocytes Compared to Cortical Neurons Due to Differential NQO1 Activity," *J Neurosci*, vol. 40, no. 23, pp. 4609–4619, Jun. 2020, doi: 10.1523/JNEUROSCI.1632-17.2020.
- [29] G. Gambino, V. Rizzo, G. Giglia, G. Ferraro, and P. Sardo, "Microtubule Dynamics and Neuronal Excitability: Advances on Cytoskeletal Components Implicated in Epileptic Phenomena," *Cell Mol Neurobiol*, Sep. 2020, doi: 10.1007/s10571-020-00963-7.
- [30] M. W. Gramlich, S. Balseiro-Gómez, S. M. A. Tabei, M. Parkes, and S. Yogev, "Distinguishing synaptic vesicle precursor navigation of microtubule ends with a single rate constant model," *Sci Rep*, vol. 11, no. 1, p. 3444, Feb. 2021, doi: 10.1038/s41598-021-82836-7.
- [31] L. G. Wright *et al.*, "Deep physical neural networks trained with backpropagation," *Nature*, vol. 601, no. 7894, pp. 549–555, Jan. 2022, doi: 10.1038/s41586-021-04223-6.
- [32] J. Zhang, W.-H. Guo, and Y.-L. Wang, "Microtubules stabilize cell polarity by localizing rear signals," *PNAS*, vol. 111, no. 46, pp. 16383–16388, Nov. 2014, doi: 10.1073/pnas.1410533111.
- [33] S. Sahu, S. Ghosh, D. Fujita, and A. Bandyopadhyay, "Live visualizations of single isolated tubulin protein self-assembly via tunneling current: effect of electromagnetic pumping during spontaneous growth of microtubule," *Sci Rep*, vol. 4, p. 7303, Dec. 2014, doi: 10.1038/srep07303.
- [34] L. Peeples, "A pulse of hope in the fight against Alzheimer's," *Proceedings of the National Academy of Sciences*, vol. 117, no. 31, pp. 18142–18145, Aug. 2020, doi: 10.1073/pnas.2013084117.
- [35] "A 'phase zero' human brain organoid platform for neuroengineering optical theranostics | NYC Neuromodulation Online 2020." https://neuromodec.com/nyc-neuromodulation-online-2020 (accessed Apr. 18, 2021).
- [36] N. Grossman et al., "Noninvasive Deep Brain Stimulation via Temporally Interfering Electric Fields," Cell, vol. 169, no. 6, pp. 1029-1041.e16, Jun. 2017, doi: 10.1016/j.cell.2017.05.024.